Remote Sensing of Environment 115 (2011) 3670–3680

Contents lists available at SciVerse ScienceDirect

Remote Sensing of Environment

journal homepage: www.elsevier.com/locate/rse

Object-based mapping of the circumpolar taiga–tundra ecotone with MODIS tree cover

K.J. Ranson [a], P.M. Montesano [b], R. Nelson [a,*]

[a] Code 614.4, Biospheric Sciences Branch, NASA/Goddard Space Flight Center, Greenbelt, Maryland 20771, USA
[b] Sigma Space Corp., Lanham, MD, 20706, USA

ARTICLE INFO

Article history:
Received 28 October 2010
Received in revised form 6 September 2011
Accepted 8 September 2011
Available online 19 October 2011

Keywords:
Taiga–tundra ecotone
MODIS
VCF
CAVM
CAPI

ABSTRACT

The circumpolar taiga–tundra ecotone was delineated using an image-segmentation-based mapping approach with multi-annual MODIS Vegetation Continuous Fields (VCF) tree cover data. Circumpolar tree canopy cover (TCC) throughout the ecotone was derived by averaging MODIS VCF data from 2000 to 2005 and adjusting the averaged values using linear equations relating MODIS TCC to Quickbird-derived tree cover estimates. The adjustment helped mitigate VCF's overestimation of tree cover in lightly forested regions. An image segmentation procedure was used to group pixels representing similar tree cover into polygonal features (segmentation objects) that form the map of the transition zone. Each polygon represents an area much larger than the 500 m MODIS pixel and characterizes the patterns of sparse forest patches on a regional scale. Those polygons near the boreal/tundra interface with either (1) mean adjusted TCC values from 5 to 20%, or (2) mean adjusted TCC values <5% but with a standard deviation >5% were used to identify the ecotone. Comparisons of the adjusted average tree cover data were made with (1) two existing tree line definitions aggregated for each 1° longitudinal interval in North America and Eurasia, (2) Landsat-derived Canadian proportion of forest cover for Canada, and (3) with canopy cover estimates extracted from airborne profiling lidar data that transected 1238 of the TCC polygons. The adjusted TCC from MODIS VCF shows, on average, <12% TCC for all but one regional zone at the intersection with independently delineated tree lines. Adjusted values track closely with Canadian proportion of forest cover data in areas of low tree cover. A comparison of the 1238 TCC polygons with profiling lidar measurements yielded an overall accuracy of 67.7%.

Published by Elsevier Inc.

1. Introduction

Earth's longest vegetation transition zone, the circumpolar taiga–tundra ecotone (TTE), stretches for more than 13,400 km around Arctic North America, Scandinavia, and Eurasia (Callaghan et al., 2002a). This ecotone is subjected to climate change (Serreze et al., 2000), and sensitive to climate change (Callaghan et al., 2002b). The shifting of local subarctic tree lines throughout the forest-tundra biome is linked to ecological processes at different spatiotemporal scales and will reflect future global climatic changes (Payette et al., 2001). Monitoring the dynamics of this forest-tundra boundary is critical for our understanding of the causes and consequences of the changes. High-latitude ecosystems, i.e. boreal forests and tundra, play an important role in the climate system (Bonan et al., 1995) and have been warming in recent decades (Chapin et al., 2005). Modeled effects of increased deciduous tree cover in high-latitudes show a positive feedback with temperature in the vegetated regions of the arctic (Swann et al., 2010). Improved understanding of the role of the forest-tundra boundary requires a concerted research effort to be conducted over a long enough time period to detect and quantify ecosystem feedbacks (Chapin et al., 2000). The objective of this study was to define a taiga-to-tundra transition zone at the northern edge of the circumpolar boreal forest to replace or augment existing tree lines in the hope that such an ecotone map might provide a more realistic benchmark for subsequent studies investigating the effects of climate change in the far north.

2. Background

The TTE is dynamic because of its sensitivity to ongoing and accelerating climate change at high latitudes. Toward the end of the last century, Arctic temperatures have risen at twice the rate of the global average, and model predictions call for an additional 4°–7 °C rise by 2100 (ACIA, 2005, pg. 10). These historically rapid temperature changes will have consequences with respect to the distribution of vegetation and carbon in the far North.

During the last 6000 years in northern Eurasia a general cooling trend of about 2–4 °C was associated with a 400–500 km southward retreat of larch and birch forest stands (Callaghan et al., 2002b). In the past three decades global average surface air temperatures have risen by approximately 0.6 °C (Hansen et al., 2006) while

* Corresponding author. Tel.: +1 301 614 6632.
E-mail address: Ross.F.Nelson@nasa.gov (R. Nelson).

0034-4257/$ – see front matter. Published by Elsevier Inc.
doi:10.1016/j.rse.2011.09.006

temperatures in parts of the Northern Hemisphere have warmed by as much as 2 °C (Hansen et al., 1999). If it is assumed that growth and reproduction are controlled by temperature, a rapid advance of the tree line would be predicted (Grace et al., 2002). The northward movement of the TTE may result if climatic warming persists over centuries or millennia (Skre et al., 2002). Some studies predict that up to about one half of the tundra could be colonized by trees by 2100 (Callaghan et al., 2002b; Harding et al., 2001).

There is general agreement that temperature is important in determining the northern extent of the boreal forest. Widespread degradation of permafrost has been shown in a number of studies (Jorgenson et al., 2006; Osterkamp & Jorgenson, 2006; Osterkamp & Romanovsky, 1996; Pavlov, 1994). Recent observations suggest that, in an indication of northern climate warming, shrubs and forests are expanding into the tundra (e.g., Blok et al., 2010; Esper & Schweingruber, 2004; Kharuk et al., 1998, 2002, 2005; Tape et al., 2006) and experimental evidence shows that increased shrub cover in the tundra is a response to warming (Walker et al., 2006). Devi et al. (2008) estimate the past century's forest expansion in the polar Ural Mountains of western Siberia has led to an increase in biomass of 40–75 Mg/ha. These observations are consistent with trends seen in northern Canada (Gamache & Payette, 2005; Laliberté & Payette, 2008; Payette & Gagnon, 1985; Payette et al., 2001).

The northern tree line response to Arctic warming is not one of monotonic expansion. Tree lines can (1) remain static (Masek, 2001; Rees et al., 2002), (2) increase in biomass and/or crown closure without moving (Payette et al., 2001; Rees et al., 2002), (3) migrate/encroach onto nonforested areas (Gamache & Payette, 2005; Rees et al., 2002), or (4) retreat, primarily in response to paludification as the permafrost melts (Crawford et al., 2003). The position of the northern portion of the boreal forest is likely influenced by a range of conditions that vary by region (Callaghan et al., 2002a; Crawford, 2005; Crawford & Jeffree, 2007).

Recent work indicates increased Arctic vegetation growth with climate warming and this growth manifests itself optically as a longer growing season, i.e., earlier green-up, later senescence, and as a greener signal, indicating increased photosynthetic activity (Myneni et al., 1997; Zhou et al., 2001). Analysis of shrub growth rings in northwestern Russian Arctic tundra has revealed field data that closely follows the patterns found in the greening signal of shrubs in the satellite record since the 1980s (Forbes et al., 2010). Results from the analysis of Landsat time series in Canada's forest–tundra interface suggest shrub replacement of bare ground and lichen cover (Olthof et al., 2008). An analysis of tree growth from 1982 to 2008 in Russia and Canada revealed a positive correlation between satellite NDVI and tree ring measurements (Berner et al., 2011).

The transition from taiga to tundra is characterized by a change in tree cover density. The TTE is not a distinct edge but a transition zone where patches of tundra and forest are mixed. It is not easily defined and can be difficult to identify and quantify, and there have been a number of remote sensing methods used to depict this ecotone (Heiskanen & Kivinen, 2008; Ranson et al., 2004; Rees et al., 2002; Timoney et al., 1992). In order to delineate this transition zone, we used the MODIS Vegetation Continuous Fields (VCF) % canopy cover product (Hansen et al., 2002, 2003).

The VCF is derived from multiple temporal composites that take advantage of spectral and phenological information to provide a percent canopy cover value for each 500 m pixel. Data from the 7 MODIS land bands are combined with NDVI and surface temperature data to generate 68 metrics from the temporal composites. These annual phenological metrics (means, maxima, minima, and amplitude of spectral information) are used as independent variables to predict

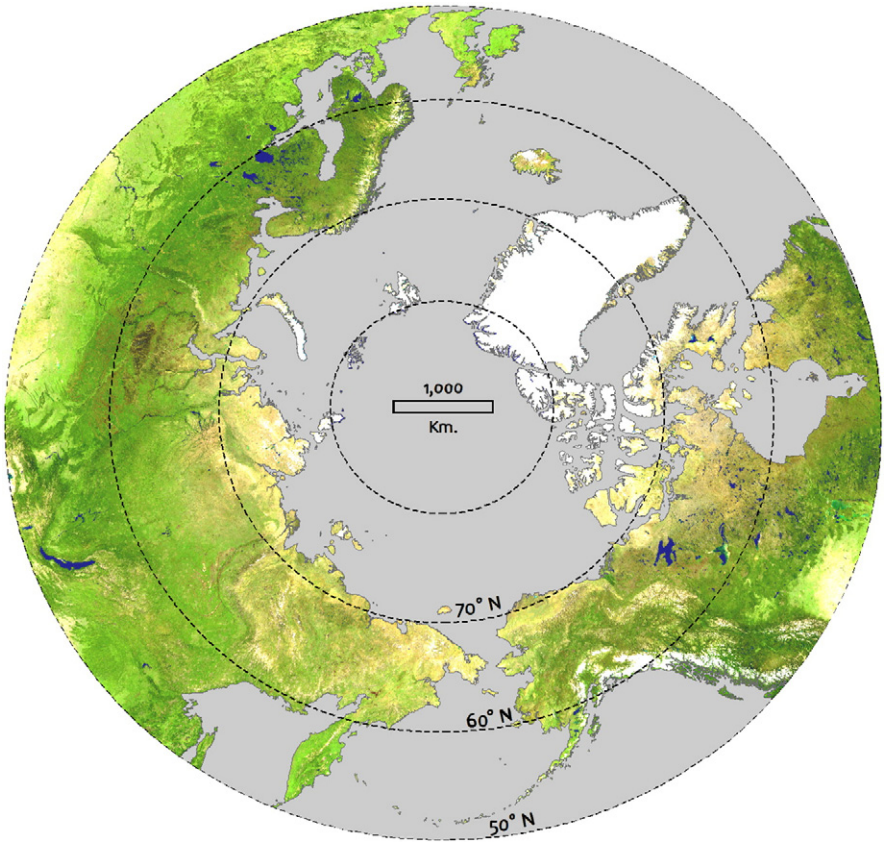

Fig. 1. MODIS true-color, cloud-free composite of the northern hemisphere in 2001. The circumpolar taiga–tundra ecotone benchmarked in this study is about 13,400 km long (Image source: NASA).

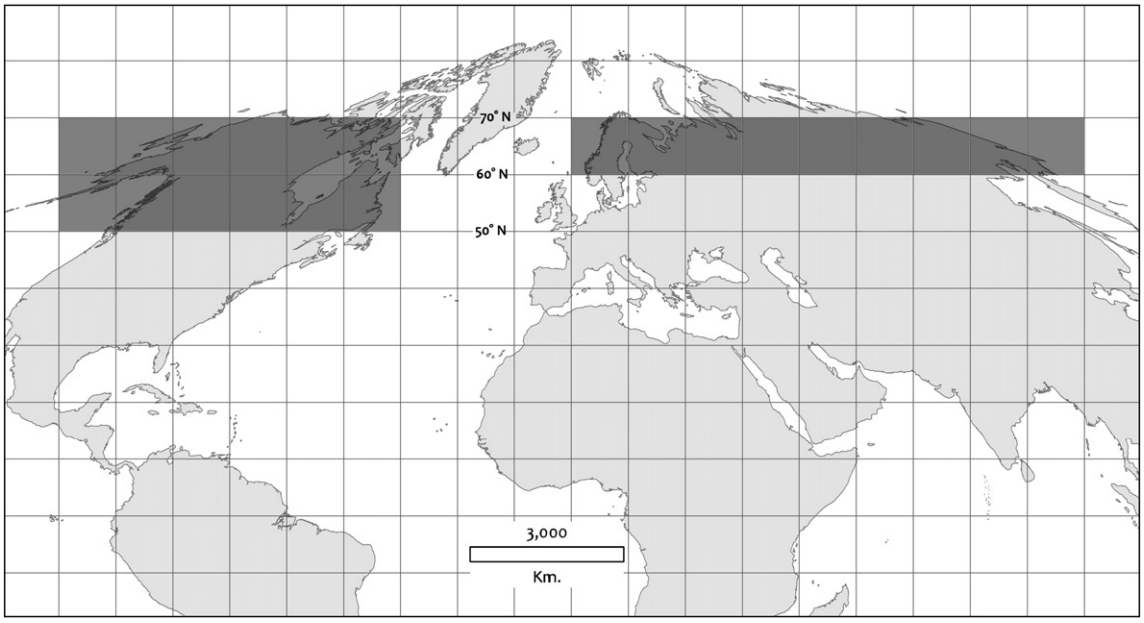

Fig. 2. The 21 Collection 4 MODIS VCF tiles gathered for continental North America and Eurasia. Each tile is 10°×10° and gridded in the sinusoidal projection.

tree cover. Continuous tree cover training sets are derived from Landsat classifications aggregated to the MODIS 500 m grid. Each coarsened 500 m value is the mean tree cover value of its higher resolution Landsat pixel components. These Landsat-derived training sets serve as the dependent variable that a fully automated regression tree predicts. The regression tree produces a continuous tree cover variable globally, without specific continental adjustments. This continuous value (0–100%) is related to the amount of skylight obstructed by tree canopies equal to or greater than 5 m in height. The heterogeneous nature of land cover at ecotone boundaries lends itself to the continuous mapping method of the VCF (Hansen et al., 2002, 2003).

3. Methods

3.1. MODIS data acquisition and processing

Fig. 1 is a composite Terra MODIS image of the northern hemisphere above 50° latitude. This image represents the geographic scope and diversity in the vegetated boreal and arctic zones. Collection 4 (C4) MODIS VCF (MOD44b) data were acquired as 10°×10° tiles for six years (2000–2005) for the 21 tiles shown in Fig. 2 through the University of Maryland's Global Land Cover Facility (http://ftp.glcf.umd.edu/data/vcf/, accessed June, 2011). Tiles for continental North America spanned 50°N–70°N and tiles for Eurasia spanned 60°N–70°N. No C4 MODIS VCF data existed above 70°N, which accounts for the data gap in northern Siberia. The data tiles were mosaicked by year for both North America and Eurasia using ENVI 4.5 software (ENVI 2010). The six years of data were then combined to derive an average VCF dataset, where each pixel represented the mean percent tree canopy cover value of the corresponding pixel across all of the six VCF yearly datasets.

3.2. VCF adjustment

Each continental multi-annual VCF mosaic was adjusted based on inversions of the results of simple linear regressions, shown in Table 1, relating Quickbird-validated percent tree canopy cover (% TCC, X variable) to MODIS VCF %TCC (Y variable). Quickbird estimates of %TCC were generated by interpreting a grid of points laid atop Quickbird images freely available in Google Earth (Montesano et al., 2009). By inverting the Table 1 equations, we could calculate, for each MODIS VCF pixel (now the X variable, after inversion), an adjustment that brings that pixel more in line with photointerpreted Quickbird estimates of %TCC. This adjustment was done primarily to mitigate a tendency of the VCF to overestimate %TCC in lightly forested regions. Though not directly related to the objectives of this study, the adjustment also stretched the upper limit of the %TCC VCF estimates from ~80%, the upper limit of the unaltered VCF standard product, to 100% (Hansen et al., 2003). The adjustments were applied for seven broad longitudinal zones representing very general circumpolar regions on a pixel-by-pixel basis (Fig. 3). A value of zero was assigned to those pixels for which the adjustment equations resulted in negative values, while a value of 100 was assigned to those pixels whose adjusted values exceeded 100% tree canopy cover. Finally, the Collection 5 MODIS land cover (MOD12Q1, IGBP global vegetation classification scheme) was used to change those VCF_{adj} pixels identified as "water" to tree canopy cover values of zero. [A second water mask is used later, in the VCF Segmentation step, to identify those VCF pixels that are ≥40% water.] Two multi-annual datasets, one for continental North America and one for Eurasia resulted from this processing sequence, each maintaining the original sinusoidal projection of the 463.3 m (nominally 500 m) pixel grid. All subsequent processing was done on these adjusted VCF values; these values are henceforth referred to as VCF_{adj}.

Table 1
Slope and y-intercept values of the linear adjustments for each circumpolar zone. Longitudes shown are the western and eastern bounds of each zone. Slope and y-intercept values based on results from Montesano et al., 2009. The simple linear models are of the form $\%TCC_{VCF} = (\text{slope})(\%TCC_{Quickbird}) + y-\text{intercept}$.

Name	Longitudinal bounds		Slope	y-intercept
	West	East		
Alaska	−180	−130	0.54	18.6
Western/Cent. Canada	−130	−80	0.53	24.58
Eastern Canada	−80	−55	0.66	10.96
Scandinavia	4	40	0.27	21.83
Western Eurasia	40	60	0.47	24.91
Central Eurasia	60	110	0.54	13.51
Eastern Eurasia	110	180	0.41	18.37

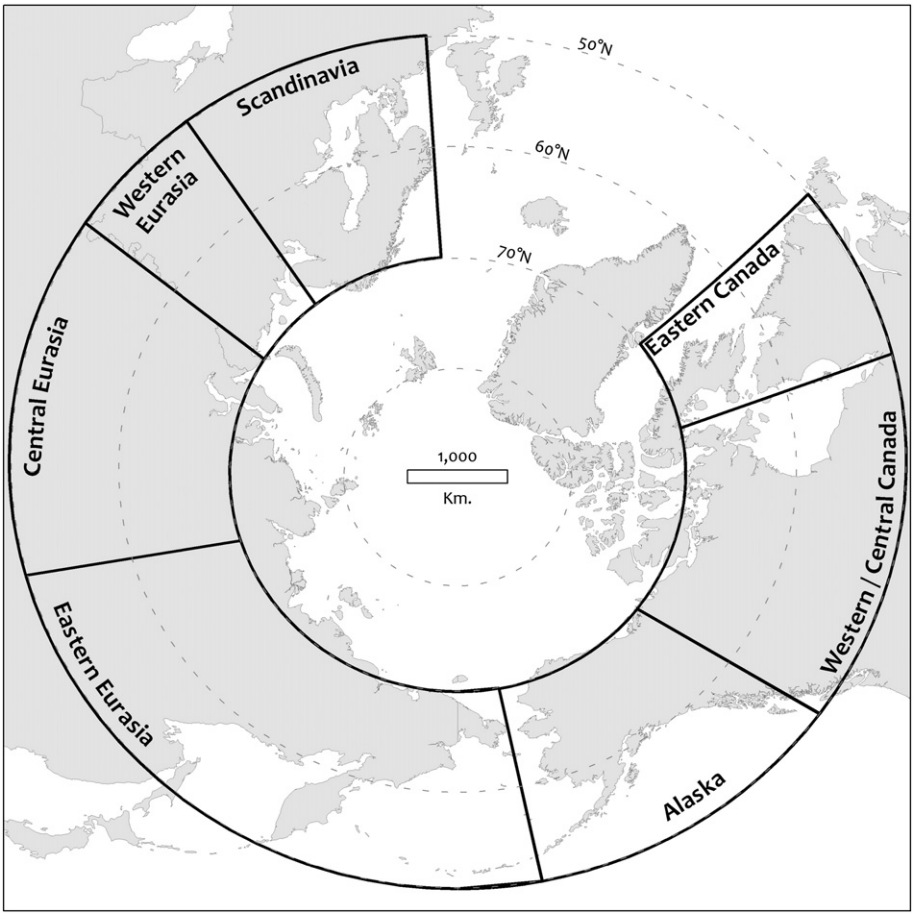

Fig. 3. The 7 circumpolar zones by which linear equations adjusting VCF tree canopy cover values were applied.

3.3. VCF segmentation

Definiens software (Definiens, 2009) was used (1) to mitigate pixel-level noise in the VCF_{adj} tree canopy cover estimates and (2) to define more homogeneous landscape units. The segmentation algorithm minimizes within-object variance by arranging groups of spectrally similar, spatially adjacent pixels into polygon image objects, hereafter referred to as polygons. The segmentation was applied to both the North American and the Eurasian VCF_{adj} mosaics. North America was divided into three tiles, where the largest was 4600 pixels × 4800 pixels, while Eurasia was divided into 5 tiles, where the largest tile was 5000 pixels × 2400 pixels.

In addition to the VCF_{adj} raster dataset, vector layer datasets were used as masks to constrain the segmentations to land areas within previously delineated taiga and tundra biomes. The World Wildlife Fund's (WWF) Global Lakes and Wetlands Database (Lehner & Doll, 2004) was used to apply a water mask to the VCF_{adj} mosaics for all water polygons labeled "lake", "river", or "reservoir" larger than 0.1 km^2. We chose to use water polygons smaller than the VCF pixel size to exclude VCF_{adj} pixels that potentially represented a mix of land and inland water. The WWF's Ecoregions (Olson et al., 2001) vector dataset depicts global terrestrial ecoregions defined as large land units comprised of distinct species and natural communities. All ecoregions within the boreal forests/taiga biome and the tundra biome were included in the vector masking portion of the overall segmentation procedure.

The segmentation process in the commercially available Definiens software involved two steps. The steps were arranged in a protocol to standardize the processing steps for each tile of the VCF_{adj}. The first step involved an initial coarse segmentation allowing the vector layers to mask portions of the VCF_{adj} land pixels that were outside the boreal forest/taiga or tundra biomes. Subsequent class assignments, masking

Table 2
Summary of the intersection of VCF_{adj} with CAVM and CAPI tree-lines. Regional longitudinal zone means are aggregated from 1° longitudinal zone means.

	Mean of all 1° long. zones		Prop. of all 1° zones <5% TC		Proportion of polygons intersecting each treeline					
					<5%		5–20%		>20%	
Name	CAVM	CAPI	CAVM	CAPI	CAVM	CAPI	CAVM	CAPI	CAVM	CAPI
Alaska	7	8	0.43	0.46	0.63	0.56	0.14	0.13	0.23	0.30
Western/Cent. Canada	<1	<1	1.00	0.97	0.98	0.98	0.01	0.02	0.01	0.00
Eastern Canada	3	6	0.69	0.56	0.86	0.68	0.13	0.26	0.00	0.06
Scandinavia	–	6	–	0.60	–	0.77	–	0.12	–	0.10
Western Eurasia	23	8	0.00	0.45	0.32	0.62	0.22	0.20	0.46	0.18
Central Eurasia	11	12	0.45	0.37	0.51	0.66	0.13	0.14	0.36	0.20
Eastern Eurasia	7	6	0.63	0.58	0.85	0.71	0.06	0.11	0.08	0.18

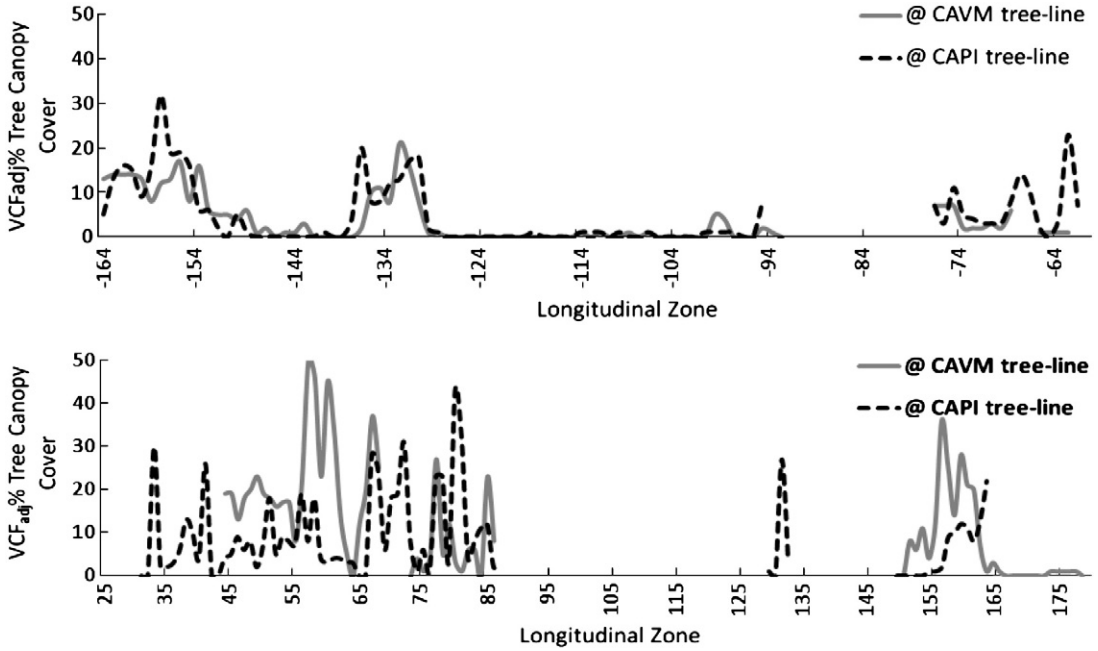

Fig. 4. (a) Mean VCF_{adj} values in each 1° longitudinal zone at the intersection with CAVM and CAPI tree lines in North America. (b) Mean VCF_{adj} values in each 1° longitudinal zone at the intersection with CAVM and CAPI tree lines in Eurasia.

and segmentations were performed based on the masks established in this first step. The second step, applied within the mask area, created polygons, i.e., image objects, based on spatial characteristics and pixel values using a consistent scale parameter and homogeneity criterion. The scale parameter guides the general size of the image objects, and depends on the homogenous nature of pixel values in an area (Baatz & Schäpe, 2000). The more homogenous the data, the larger the objects tend to be. The goal of this segmentation procedure was (1) to construct polygons that represented various tree cover (forest) patches, (2) to identify contiguous gaps with little or no tree cover, and (3) to delineate polygons with varying tree cover densities. The homogeneity criterion is comprised of complementary color and shape components. A weight of 0.8 was given to the Definiens component called color, which in this case is derived from the digital value of the VCF_{adj}. The Definiens shape component, which defines the textural homogeneity of the resulting image objects, received the remaining 20% (Definiens, 2009).

3.4. Taiga–tundra ecotone mapping

The mapping portion was accomplished by classifying polygons based on a specified range of VCF_{adj} values that represent the TTE. The mean and standard deviation of the VCF_{adj} pixel values within each polygon were calculated. Polygons, whose sizes ranged widely depending on the homogeneity of local VCF_{adj} values, were considered part of the TTE if they fit one of the following two criteria:

1. The mean VCF_{adj} value from 5% through 20% (5–20%).
2. The mean VCF_{adj} value was <5% and the standard deviation >5%.

We consider those polygons in the 5–20% class as the core of the TTE. The second class represents more of a transition from lightly forested areas to no trees. Sections within these Class 2 polygons might have been identified as part of the core areas had different

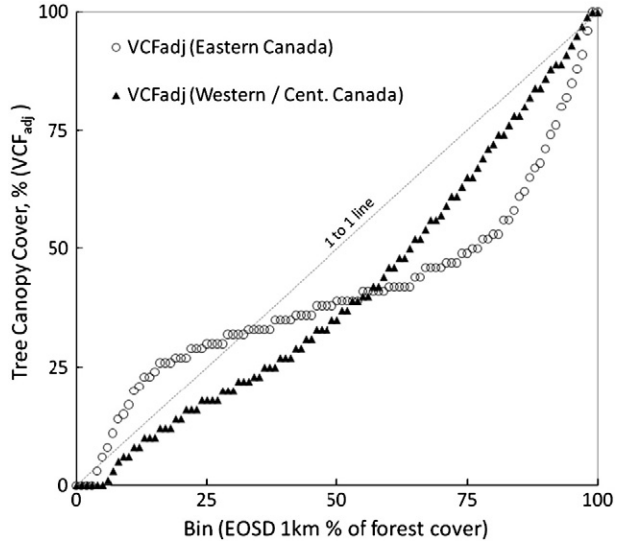

Fig. 5. The median value of VCF_{adj} %TCC for each bin of EOSD proportion of forest at 1% intervals.

Table 3
Laser-based estimates of percent tree canopy cover versus VCF_{adj} polygon averages for 1238 polygons in the taiga/tundra region of the North American boreal forest.

	Airborne profiling LiDAR			
VCF_{adj}	Tundra	TTE	Boreal forest/taiga	# of polygons
Tundra	162	68	12	242
TTE	34	176	50	260
Boreal forest/taiga	11	225	500	736
# of polygons	207	469	562	1238

	PA	UA	O	C
Tundra	78.26%	66.94%	21.74%	33.06%
TTE	37.53%	67.69%	62.47%	32.31%
Boreal forest/taiga	88.97%	67.93%	11.03%	32.07%

PA = producer's accuracy
UA = User's accuracy
C = error of commission
O = error of omission

Overall accuracy =	67.69%
Khat =	0.4771

segmentation criteria been used to partition the ecotone. We hypothesize that these Class 2 areas might be viewed as the colonization areas, areas at the forefront of vegetation encroachment onto the treeless tundra or, alternatively, vegetation dieback due to paludification. Values within the biomes "boreal forest/taiga" and "tundra" that did not meet these criteria were not considered part of the TTE. Image objects whose mean adjusted value and standard deviation were both less than 5% were considered outside the TTE

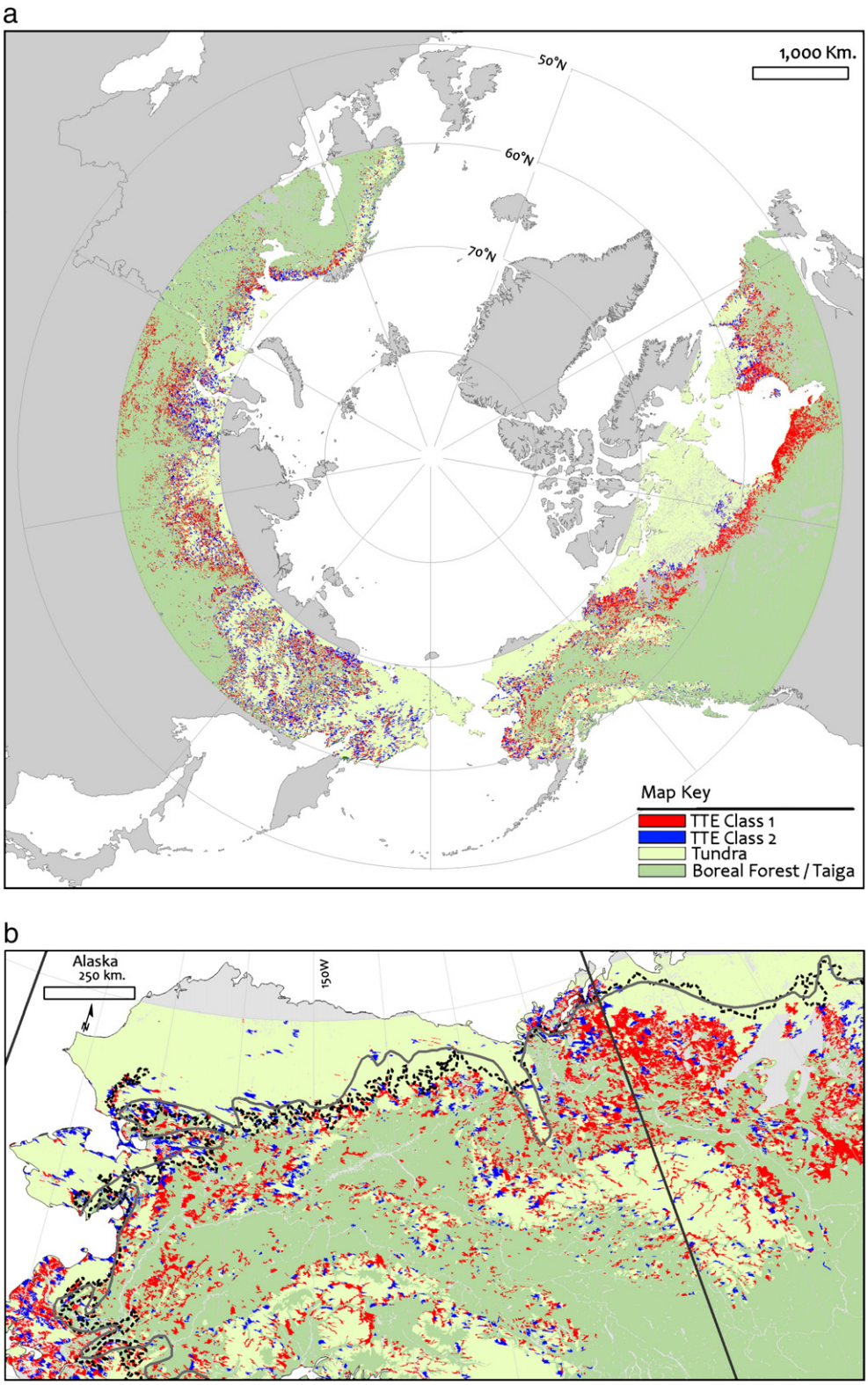

Fig. 6. The circumpolar taiga–tundra ecotone (TTE) map (a). TTE Class 1 (red) depicts areas with a mean of 5–20% tree canopy cover and TTE Class 2 (blue) depicts areas of tree canopy cover <5% and standard deviation >5%. Dark green areas identify the boreal forest ecozone, light green areas are nonforest/ice/rock/tundra, and gray areas are those above 70°N (no Collection 4 MODIS VCF data) or below 60° (Eastern Hemisphere) or 50° (Western Hemisphere). (b–g) depict larger scale versions of the 6a map, beginning in Alaska and moving to the east. CAVM and CAPI treelines are shown as solid gray and dotted black lines, respectively.

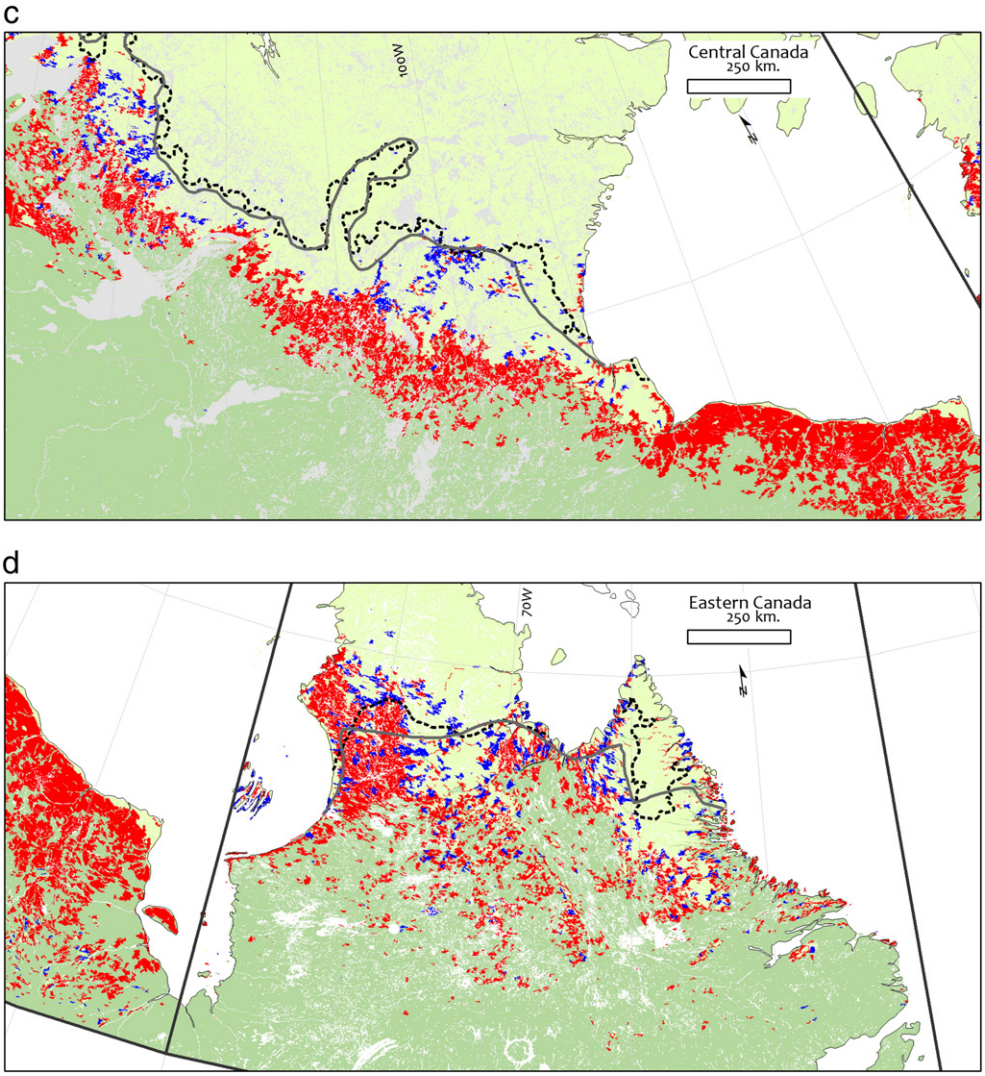

Fig 6 (*continued*).

and classified as tundra while image objects with a mean VCF_{adj} value greater than 20% were not considered part of the TTE and were classified as boreal forest.

3.5. Assessing the accuracy of the TTE–VCF_{adj} map

Assessing the accuracy of the TTE product is challenging given the inaccessibility of the circumpolar TTE and the paucity of generally accepted, quality-checked, independent ecotone and tree line maps. In this study we compared our TTE VCF_{adj} map to four independent data sources that contain information concerning the northern extent of the boreal forest:

(1&2). Comparison to Established Tree Lines: The TTE VCF_{adj} percent tree canopy cover pixel values are compared to two circumpolar, vector lines that approximate the northern limit of trees. These two very general tree line depictions derive tree line from a variety of regional-global scale sources. The Circumpolar Arctic Vegetation Map (CAVM) (Walker et al., 2005) and the Circum-Arctic Map of Permafrost and Ground-Ice Conditions (CAPI) (Heginbottom et al., 1993) were decomposed into points at intervals of ~463 m (the size of a VCF pixel). These points were used to sample corresponding VCF_{adj} pixels within one-degree longitudinal intervals wherever the points overlay VCF_{adj} pixels. The VCF pixel-sized interval was used to avoid sampling any single VCF pixel more than once. For each 1° interval, the mean VCF_{adj} value for all VCF_{adj} pixels intersecting the sampling points from both the CAVM and the CAPI tree lines were used to determine the mean VCF_{adj} TCC at each tree line.

(3). Comparison to a Landsat ETM + derived Proportion of Forest Cover Map of Canada: The VCF_{adj} canopy cover map was compared to a forest cover proportion map developed by the Canadian Forest Service of Natural Resources Canada. The dataset is a 1 km product aggregated from the 25 m Landsat-based EOSD (Earth Observation for Sustainable Development) land cover map of Canada (Wulder et al., 2008). The value of each 1 km grid cell represents the proportion of the cell occupied by the within-cell modal EOSD class. The dataset was provided in the Lambert Conformal Conic projection and was resampled to the sinusoidal projection to match that of the VCF. It covers nearly 6.6 million km^2, approximately 1.7 million of which lie in the Eastern Canada zone and 4.9 of which lie in the Western Canada zone. The dataset accounts for nearly one third of the world's boreal forest, and one tenth of the global forest cover. For the two broad circumpolar zones in which Canada lies, a zonal mean analysis was performed to compare proportion of forest values at 1 km (from EOSD) to mean TCC values from the VCF_{adj}. For each EOSD value from 0 to 100% forest cover, we computed the median VCF_{adj}.

(4). Comparison to Airborne Profiling Lidar Measurements: The TTE VCF_{adj} values were compared to airborne laser measurements of canopy closure. Seventeen trans-boreal airborne profiling laser flight

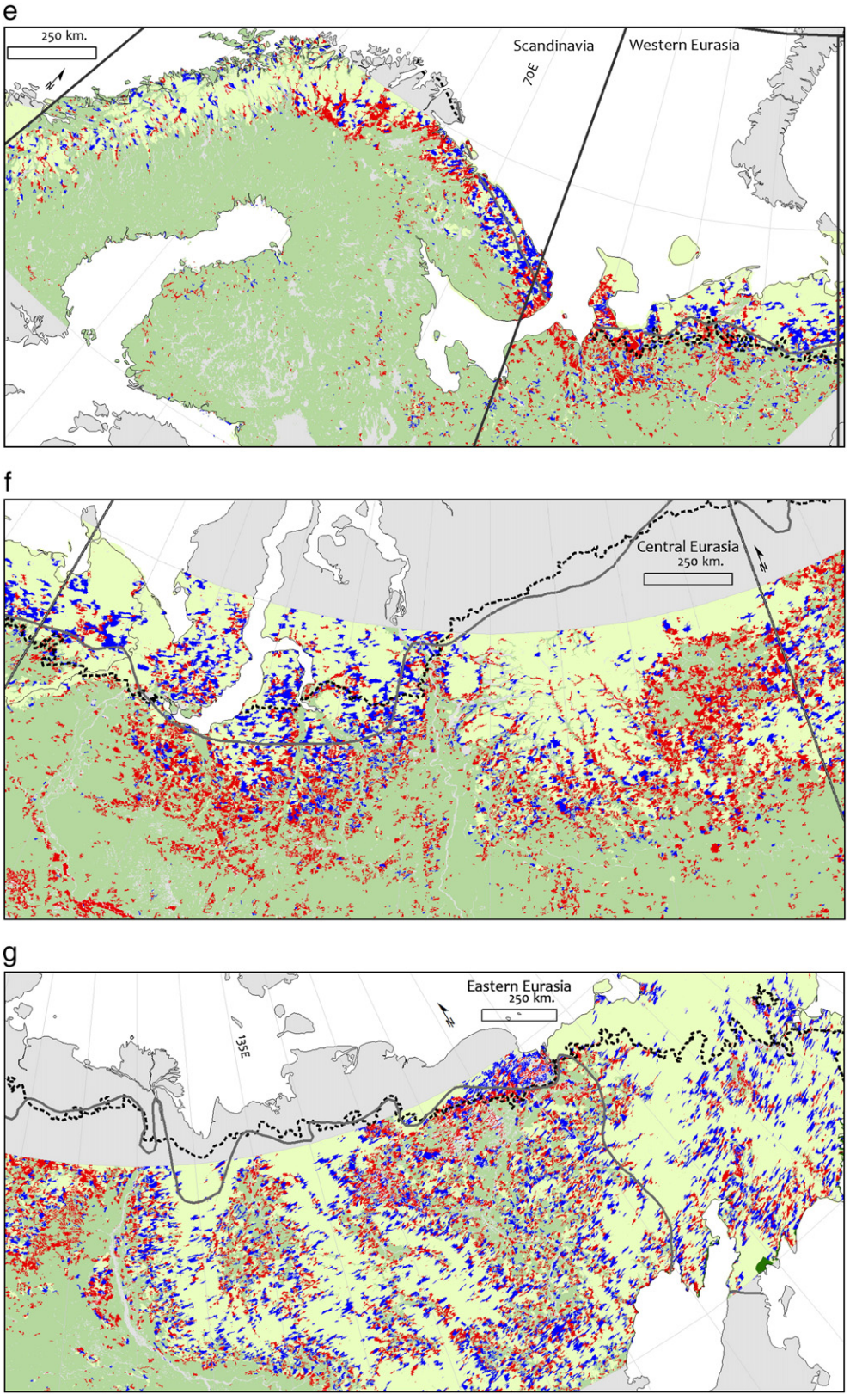

Fig 6 (*continued*).

lines were collected across Alaska and Canada between 2005 and 2009 — 2 in Alaska (2008), 11 in western and central Canada (2009), and 4 in Quebec (2005). Given the definition of a tree with respect to laser height characteristics, it is a straightforward exercise to parse profiling laser pulses into canopy and non-canopy hits along segments 30 m long. The 30 m segment length was selected to be as short as possible while still insuring that there would be ≥50 laser pulses, i.e., observations of canopy height, within a given segment. Lidar data capture rates varied from 140 Hz to 333 Hz, depending on the flight mission; the nominal speed of the aircraft was

~50 m s^{-1} (180 km h^{-1}, or ~100 kn). Lidar-based estimates of percent canopy cover are compared with VCF_{adj} estimates for 1238 polygons intercepted in and adjacent to the TTE within WWF ecozones identified as taiga or tundra at the northern edge of the North American boreal forest.

For the purposes of this investigation, a lidar ranging measurement was considered to have intercepted a tree canopy if that canopy height measurement was greater than 1.3 m above the ground. This minimum tree height measurement was selected because it yielded lidar canopy closure estimates that, when used to predict VCF_{adj} polygon values, yielded a slope of one. In essence, we tuned the lidar measurements, as best we could, to reproduce VCF_{adj} estimates. We note that Hansen et al. (2002) define a tree as any green vegetation greater than 5 m tall. With a profiling lidar we cannot adopt the same measurement because Hansen's 5 m height value refers to the top height of a tree. A profiling lidar will rarely hit/measure the tops of the trees along a flight transect; the vast majority of pulses along a segment will measure the shoulders of trees or, in a sparse boreal transition zone, ground.

4. Results

4.1. Accuracy of the VCF_{adj} TTE map

(1&2). Comparison to Established Tree Lines: The intersection of VCF_{adj} polygons with two representations of tree-line was produced for the circumpolar ecotone below 70°N. The intersection of the datasets shows the correspondence of low VCF_{adj} %TCC values with tree-line in North America and Eurasia compiled for each regional zone (Table 2). The regional zone means are an aggregation of the 1° longitudinal means of the VCF_{adj} values at their intersection with each tree-line. Adjusted values above 20% are reported for the Western Eurasia regional zone (40°E–60°E), while all other zones average less than 12% VCF_{adj} tree cover at both tree-lines. Most of the regional zones have a mean %TCC less than 5 for at least 40% of their 1° intervals (5 of 6 of the zones at the CAVM tree line, 6 of 7 at the CAPI tree line). This is indicative of agreement among the tree line data and the VCF_{adj} on areas of low %TCC.

Plots of mean VCF_{adj} values for each 1° longitudinal zone in North America (Fig. 4a) and Eurasia (Fig. 4b), show the performance of the VCF_{adj} across the circumpolar transition zone. In North America, particularly west of Hudson Bay, the linear adjustments brought %TCC values to near zero in many longitudinal zones. In Eurasia, VCF_{adj} values are more variable, and spikes in %TC are apparent between 55°E and 80°E. There is a broad gap in Fig. 4b between 88°E and 148°E where, for the most part, the CAVM and CAPI tree-lines lie above 70°N, where C4 VCF data were not available. An interruption of the intersection between the tree lines and the VCF_{adj} also occurs in North America at Hudson Bay.

(3). Comparison to a Landsat ETM + Percent Forest Cover Map of Canada: We compared the VCF_{adj} to the EOSD-derived proportion of forest within a 1 km × 1 km grid cell. The median VCF_{adj} value associated with each EOSD 1% bin was plotted for both of Canada's regional zones (Fig. 5). Although the VCF_{adj} values range from 0% to 100% for all EOSD bins, the median VCF_{adj} is within an average of 5% TCC between EOSD bins 0–30 for both Eastern and Western Canada. The low %TCC portion of the plot is of particular interest because the adjustment algorithms applied to the VCF were designed for areas of low TCC.

The EOSD–VCF_{adj} comparison illustrated in Fig. 5 is an approximation because the two products are responding to two different definitions of forest. The VCF_{adj} map depicts information about a continuous variable, %TCC, from 0 to 100% that has been grouped into classes. The EOSD data depicts the proportion of the 1 km^2 cell occupied by smaller 30-meter EOSD pixels classified as forest.

(4). Comparison to Airborne Profiling Lidar Measurements: Table 3 reports various accuracy measures associated with airborne profiling lidar measurements made on 1238 polygons within the North American taiga and tundra ecozones. A polygon-level confusion matrix is provided as well as common accuracy measures. Tundra identifies those polygons with average VCF_{adj} values below 5% tree canopy cover with standard deviations <5%. The TTE class includes the 0–5% VCF_{adj} class with standard deviations >5% and the 5–20% class. Forest identifies those polygons with VCF_{adj} values >20%.

In this presentation, the lidar measurements are considered the reference data set, however we stress again that we can generate any variety of numbers by adjusting our lidar definition of a pulse intercepting a tree. In Table 3, the numbers reflect a definition where every laser pulse that measures a height >1.3 m above the ground is considered to have hit a tree. Increasing this laser-based minimum canopy height would essentially "push" the confusion matrix polygon counts into less dense laser canopy closure classes, i.e., polygon counts in map classes would increase to the left in Table 3 as the laser-based minimum canopy height increased, with the row sum remaining constant. However the counts reported in Table 3 are those that most closely reflect VCF_{adj} polygon averages; witness the fact that the slope of the scatterplot of VCF_{adj} versus profiling lidar canopy closure equals one at a minimum laser canopy height of 1.3 m.

The overall accuracy of the TTE map when compared to laser measurements is 67.7%, with a much lower Khat value of 0.48, reflective of the high omission error rate of 62.5% and the complementary 37.5% producers accuracy statistic for the TTE class. This omission error and the polygon counts for the TTE class suggests that, at least with respect to laser measurements, our VCF map has a propensity to identify TTE polygons as forest, i.e., >20% tree canopy cover. The user's accuracy for the TTE, conversely, suggests that if a polygon is identified on the TTE map as being in the TTE, then 67.7% of the time, that polygon is correctly identified.

4.2. The circumpolar taiga–tundra ecotone map

The map delineates a global scale circumpolar taiga–tundra ecotone for the base period 2000–2005. The map data are cast in the sinusoidal projection, matching the original projection of the input VCF. In Eurasia, the map extends from 60°N to 70°N, and in North America from 50°N to 70°N, excluding Baffin Island in northeastern Canada and the Aleutian Peninsula in southwestern Alaska. Fig. 6a shows the map of the circumpolar TTE in a polar projection. Fig. 6b–g shows greater detail for each regional zone. These regional maps highlight the variability of the ecotone between regions as well as the patchy nature of the TTE and the relationship between the TTE polygons and two tree-lines.

The data exists in digital GIS format, as both raster GeoTiff files and vector shapefiles. The vector shapefiles contain mean and standard deviation VCF_{adj} percent tree canopy cover values for each ecotone polygon, as well as the area of each polygon in square kilometers. The ecotone is delineated with two classes. Class 1 is comprised of polygons of 5%–20% mean tree canopy cover. Polygons with less than 5% mean tree canopy cover but with a standard deviation greater than 5% make up Class 2. The minimum size for 95% of the TTE polygons is 2.5 km^2, which corresponds to the minimum mapping unit. Greater than 95% of the area mapped as ecotone is comprised of polygons that are at least 20 km^2 in size.

The ecotone, below 70°N, covers over 1.9 million km^2, 64% of which is found in North America. Table 4 summarizes the area of each ecotone class by regional zone. Regional ecotone areas range widely from 49,000 to 322,000 km^2 in Class 1 and from 33,000 to 301,000 km^2 in Class 2. This may be largely due to the longitudinal extent of each zone.

5. Discussion

We use adjusted values of continuous tree canopy cover from the MODIS VCF to map the ecotone at the taiga–tundra interface. The

Table 4
Area of both circumpolar ecotone classes broken down by regional zone. TTE Class 1 includes polygons with tree canopy cover of 5%–20%. TTE Class 2 includes polygons with <5% mean tree canopy cover and with a standard deviation of >5% mean tree canopy cover.

Name	Area (km^2)	
	TTE Class 1	TTE Class 2
Alaska	183,846	83,307
Western/Cent. Canada	305,032	35,756
Eastern Canada	123,155	35,172
Scandinavia	49,029	35,333
Western Eurasia	53,389	32,694
Central Eurasia	269,404	119,007
Eastern Eurasia	322,080	300,842

VCF_{adj} values were segmented and the segments then further grouped into %TCC classes. These classes are bounded by a maximum %TCC of 20%. This upper bound is consistent with the definition of the lower limit of forest in Potapov et al. (2008), where global intact forest landscapes were mapped using VCF TCC above 20%. The purpose of the segmentation process was to reduce pixel-level scatter, and derive patches of low tree canopy cover. While patches of low VCF_{adj} TCC do not necessarily indicate an ecotone, their proximity to the boundary of the boreal forest/taiga and tundra biomes help define the collective meaning of groups of patches. These groups of patches illustrate the complex regional variations in the transition from forest to tundra, and identify the circumpolar taiga–tundra ecotone for the 2000–2005 base period.

The circumpolar taiga–tundra ecotone map shows regional differences across both North America and Eurasia. In the Central Canada zone (west of Hudson Bay), the map depicts an ecotone that is relatively well defined. In this zone, ecotone polygons coalesce revealing a visually identifiable, rapid NE–SW transition of patches of homogenous low tree canopy cover. The steep vegetation gradients of this portion of the ecotone, well documented in Timoney et al. (1992) and Payette et al. (2001), are due to elevation changes, parent material and fire history. Timoney et al. (1992) indicate that changes in the width of the ecotone in Canada are also correlated with radiation, climate, and edaphic conditions. The ecotone east of Hudson Bay is more discontinuous, possibly due to trees' difficulty in reproducing after disturbances (ACIA, 2005; Payette & Gagnon, 1985). Other portions of the circumpolar ecotone, such as the Eastern Eurasia zone, reveal a more fragmented environment where the transition from closed canopy forest to open tundra at the regional scale is primarily driven by topography.

The comparison of the CAVM and CAPI tree lines with the VCF_{adj} shows the level of agreement between these two representations of the northern extent of tree cover. Since the segmented MODIS-resolution map cannot delineate a tree line, we acknowledge the inherent difficulty in comparing the CAVM and CAPI lines with polygons based on groups of 500 m pixels. Our method of sampling the VCF_{adj} using points along each tree line spaced at a distances equal to the width of a MODIS pixel provides one measure of the performance of the VCF_{adj} at 1° longitudinal intervals. The low mean values in Canada and the relatively higher values in Eurasia are not surprising. The Canadian ecotone is more compact and thus easier to depict with a line. Sections of the ecotone that are more fragmented are less likely to have an easily identifiable tree line. Landscape fragmentation may account for the preponderance of the spikes in mean VCF_{adj} values in the 1° zones in Western Eurasia. Spikes may also be due to artifacts of the adjustment. The linear adjustment algorithms were designed to reduce the overestimations of tree canopy cover in areas of low TCC. Where the VCF did not initially identify low tree cover, the VCF_{adj} will show increased %TCC values. This may be occurring in some the longitudinal zones showing spikes in VCF_{adj} relationship with tree line data. These areas should be considered for more local scale refinement. Furthermore, latitude may not be the primary determinant constraining the ecotone throughout the region. Geographic features such as river corridors traversing a north–south gradient through the ecotone may account for significant variations in local tree cover conditions.

Although the VCF maps tree canopy cover, there is evidence that the VCF TCC product confuses trees with shrubs (Gessner et al., 2008; Heiskanen, 2008; Montesano et al., 2009). As the Arctic warms, the increase in shrub cover that is correlated to a greening signal, described by Forbes et al. (2010), may be inadvertently documented by the VCF. The adjustment of the VCF addresses the confusion between shrub and tree cover greater than 5 m (Hansen et al., 2003), however some shrub/tree confusion most likely persists.

The C4 VCF data gap above 70°N presents a problem where the ecotone extends above this latitude. There are several areas above 70°N where visual inspection of high-resolution multispectral imagery reveals forested patches, e.g., northern Scandinavia and Russia's Taimyr Peninsula and Yana River Delta. Documenting these portions of the ecotone is critical but such analysis will have to await the availability of an updated VCF product that will include the processing of MODIS tiles above 70°N.

This TTE map can be a used in a number of ways. First, it can be included in global models that require forest extent information for the high northern latitudes. The map provides an explicit, area-based northern edge of most of the boreal forest/taiga. Second, when used as a mask, the map identifies areas of sparse forest patches across a broad scale where researchers may expect rapid and variable vegetation changes to occur at forest fronts. The TTE is derived from 500 m pixels, a spatial resolution appropriate to measuring/mapping global phenomena, but perhaps too large to serve to monitor vegetation changes that take place on the scale of kilometers over decades. As such, the TTE map may be employed in data integration/fusion studies to target areas that have high potential for change and areas that should be studied with finer resolution radar and lidar data to measure forest patch- and gap-level 3-D vegetation structure.

6. Conclusions

We mapped the circumpolar taiga–tundra ecotone using 500 m MODIS VCF data from 2000 to 2005 adjusted to improve tree canopy cover delineation in areas of low tree cover. The map provides an estimation of the transition between boreal forest/taiga and tundra and serves as benchmark for subsequent monitoring. We mapped the ecotone from 50°N to 70°N in North America and from 60°N to 70°N in Eurasia with polygons of VCF_{adj} tree canopy cover below 20%. The internal composition of each polygon is characterized by mean and variance values that explain the heterogeneity of the VCF_{adj} pixels that form the polygon classes of tree cover. The first class, covering >1.3 million km^2 represents 5–20% adjusted tree canopy cover. The second class, covering >0.6 million km^2 represents patches of adjusted tree canopy cover <5% with standard deviations >5%. The minimum mapping unit is approximately 2.5 km^2, which is the minimum size of 95% of the Classes 1 and 2 ecotone polygons. Groups of polygons reveal the variability of the ecotone across 7 regional zones. The consistent treatment of the entire circumpolar region using objective, repeatable image processing methods facilitates (1) comparisons among regions and (2) use with other global datasets.

Acknowledgments

This work was supported by the NASA's Earth Science Division as part of the International Polar Year program.

References

ACIA (2005). *Impacts of a warming Arctic: Arctic climate impact assessment.* Cambridge: Cambridge University Press.

Baatz, M., & Schäpe, A. (2000). Multiresolution segmentation: an optimizing Approach for high quality multi-scale image segmentation. In J. Strobl, & T. Blaschke (Eds.), *Angewandte Geographisch Informationsverarbeitung, XII*. Heidelberg: Wichmann.

Berner, L. T., Beck, P. S. A., Bunn, A. G., Lloyd, A. H., & Goetz, S. J. (2011). High-latitude tree growth and satellite vegetation indices: Correlations and trends in Russia and Canada (1982–2008). *Journal of Geophysical Research*, *116*, 1–13 G01015.

Blok, D., Heijmans, M., Schaepman-Strub, G., Kononov, A. V., Maximov, T. C., & Berendse, F. (2010). Shrub expansion may reduce summer permafrost thaw in Siberian tundra. *Global Change Biology*, *16*, 1296–1305.

Bonan, G. B., Chapin, F. S., III, & Thompson, S. L. (1995). Boreal forest and tundra ecosystems as components of the climate system. *Climate Change*, *29*, 145–167.

Callaghan, T. V., Crawford, R. M. M., Eronen, M., Hofgaard, A., Payette, S., Rees, W. G., et al. (2002). The dynamics of the tundra–taiga boundary: An overview and suggested coordinated and integrated approach to research. *Ambio*, 3–5.

Callaghan, T. V., Werkman, B. R., & Crawford, R. M. M. (2002). The tundra–taiga interface and its dynamics: Concepts and applications. *Ambio*, 6–14.

Chapin, F. S., III, McGuire, A. D., Randerson, J., Pielke, R., Sr., Baldocchi, D., Hobbie, S. E., et al. (2000). Arctic and boreal ecosystmes of western North America as components of the climate system. *Global Change Biology*, *6*(1), 211–223.

Chapin, F. S., III, Sturm, M., Serreze, M. C., McFadden, J. P., Key, J. R., Lloyd, A. H., et al. (2005). Role of land-surface changes in Arctic summer warming. *Science*, *310*, 657–660.

Crawford, R. M. M. (2005). Trees by the sea: Advantages and disadvantages of oceanic climates. *Proceedings of the Royal Irish Academy*, *105B*, 129–139.

Crawford, R. M. M., & Jeffree, C. E. (2007). Northern climates and woody plant distribution. In J. B. Orbaek, R. Kallenborn, I. Tombre, E. N. Hegseth, S. Falk-Petersen, & A. H. Hoel (Eds.), *Arctic-alpine ecosystems and people in a changing environment* (pp. 85–104). Berlin: Springer Verlag ISBN-10 3-540-48512-4 and ISBN-13 978-3-540-48512-4.

Crawford, R. M. M., Jeffree, C. E., & Rees, W. G. (2003). Paludification and forest retreat in northern oceanic environments. *Annals of Botany*, *91*(2), 213–226, doi:10.1093/aob/mcfl85.

Definiens (2009). *eCognition Developer 8 User Guide*. Munich, Germany: Definiens AG.

Devi, N., Hagedorn, F., Moiseev, P., Bugmann, H., Shiyatov, S., Mazepa, V., et al. (2008). Expanding forests and changing growth forms of Siberian larch at the Polar Urals treeline during the 20th century (pages 1581–1591). *Global Change Biology*, *14* (7), 1455–1702, doi:10.1111/j.1365-2486.2008.01583.x.

Esper, J., & Schweingruber, F. H. (2004). Large-scale treeline changes recorded in Siberia. *Geophysical Research Letters*, *31*, 1–5.

Forbes, B. C., Fauria, M. M., & Zetterberg, P. (2010). Russian Arctic warming and 'greening' are closely tracked by tundra shrub willows. *Global Change Biology*, *16*, 1542–1554.

Gamache, I., & Payette, S. (2005). Latitudinal response of subarctic tree lines to recent climate change in eastern Canada. *Journal of Biogeography*, *32*, 849–862.

Gessner, U., Conrad, C., Hüttich, C., Keil, M., Schmidt, M., Schramm, M., et al. (2008). A multi-scale approach for retrieving proportional cover of life forms. *IEEE International Geoscience and Remote Sensing Symposium* (pp. 700–703).

Grace, J., Berninger, F., & Nagy, L. (2002). Impacts of climate change on tree line. *Annals of Botany*, *90*(4), 537–544.

Hansen, M. C., Defries, R., Townshend, J., Carroll, M., Dimiceli, C., & Sohlberg, R. (2003). Global percent tree cover at a spatial resolution of 500 meters: First results of the MODIS vegetation continuous fields algorithm. *Earth Interactions*, *7*, 1–15.

Hansen, M. C., DeFries, R. S., Townshend, J. R. G., Sohlberg, R., Dimiceli, C., & Carroll, M. (2002). Towards an operational MODIS continuous field of percent tree cover algorithm: Examples using AVHRR and MODIS data. *Remote Sensing of Environment*, *83*, 303–319.

Hansen, J., Ruedy, R., Glascoe, J., & Sato, M. (1999). GISS analysis of surface temperature change. *Journal of Geophysical Research*, *104*, 30997–31022, doi:10.1029/1999JD900835.

Hansen, J., Sato, M., Ruedy, R., Lo, K., Lea, D. W., & Medina-Elizade, M. (2006). Global temperature change. *Proceedings of the National Academy of Sciences*, *103*(39), 14288–14293.

Harding, R. J., Gryning, S. E., Halldin, S., & Lloyd, C. R. (2001). Progress in understanding of land surface/atmosphere exchanges at high latitudes. *Theoretical and Applied Climatology*, *70*, 5–18.

Heginbottom, J. A., Brown, J., Melnikov, E. S., & Ferrians, O. J., Jr. (1993). Circum-arctic map of permafrost and ground ice conditions. *Proceedings of the Sixth International Conference on Permafrost. Wushan, Guangzhou, China: South China University Press*, *vol. 2*. (pp. 1132–1136) Boulder, CO: National Snow and Ice Data Center/World Data Center for Glaciology Revised December 1997.

Heiskanen, J. (2008). Evaluation of global land cover data sets over the taiga–tundra transition zone in northernmost Finland. *International Journal of Remote Sensing*, *29*(13), 3727–3751.

Heiskanen, J., & Kivinen, S. (2008). Assessment of multispectral, -temporal and -angular MODIS data for tree cover mapping in the tundra–taiga transition zone. *Remote Sensing of Environment*, *112*, 2367–2380.

Jorgenson, M. T., Shur, Y. L., & Pullman, E. R. (2006). Abrupt increase in permafrost degradation in Arctic Alaska. *Geophysical Research Letters*, *33*, L02503, doi: 10.1029/2005GL024960.

Kharuk, V. I., Dvinskaya, M. L., Ranson, K. J., & Im, S. T. (2005). Expansion of evergreen conifers to the larch-dominated zone and climatic trends. *Russian Journal of Ecology*, *36*(3), 164–170.

Kharuk, V. I., Ranson, K. J., Tret'yakova, V., & Shashkin, E. A. (2002). Reaction of the larch dominated communities on climate trends. In L. E. Paques (Ed.), *Proceedings of an International Symposium "Improvement of Larch (Larix sp.) for better growth, stem form and wood quality". France Gap, September 16–21* (pp. 289–295). : INRA.

Kharuk, V. I., Shiyatov, S. G., Naurzbaev, M. M., & Fedotova, E. V. (1998). Forest–tundra ecotone response to climate change. In Severin Woxhott (Ed.), *Proceeding of IBFRA-98* (pp. 19–23). Oslo, Norway: Oslo Sept 21–23.

Laliberté, A. C., & Payette, S. (2008). Primary succession of subarctic vegetation and soil on the fast-rising coast of eastern Hudson Bay, Canada. *Journal of Biogeography*, *35*, 1989–1999.

Lehner, B., & Doll, P. (2004). Development and validation of a global database of lakes, reservoirs and wetlands. *Journal of Hydrology*, *296*, 1–22.

Masek, J. G. (2001). Stability of boreal forest stands during recent climate change: Evidence from Landsat satellite imagery. *Journal of Biogeography*, *28*, 967–976.

Montesano, P. M., Nelson, R., Sun, G., Margolis, H., Kerber, A., & Ranson, K. J. (2009). MODIS tree cover validation for the circumpolar taiga–tundra transition zone. *Remote Sensing of Environment*, *113*, 2130–2141.

Myneni, R. B., Keeling, C. D., Tucker, C. J., Asrar, G., & Nemani, R. R. (1997). Increased plant growth in the northern high latitudes from 1981 to 1991. *Nature*, *386* (6626), 698–702.

Olson, D. M., Dinerstein, E., Wikramanayake, E. D., Burgess, N. D., Powell, G. V. N., Underwood, E. C., et al. (2001). Terrestrial ecoregions of the worlds: A new map of life on Earth. *Bioscience*, *51*, 933–938.

Olthof, I., Pouliot, D., Latifovic, R., & Chen, W. J. (2008). Recent (1986–2006) vegetation-specific NDVI trends in Northern Canada from satellite data. *Arctic*, *61*, 381–394.

Osterkamp, T. E., & Jorgenson, J. C. (2006). Warming of permafrost in the Arctic National Wildlife Refuge, Alaska. *Permafrost and Periglacial Processes*, *17*, 65–69.

Osterkamp, T. E., & Romanovsky, V. E. (1996). Characteristics of changing permafrost temperatures in the Alaskan Arctic, USA. *Arctic and Alpine Research*, *28*(3), 267–273.

Pavlov, A. V. (1994). Current changes of climate and permafrost in the arctic and subarctic of Russia. *Permafrost and Periglacial Processes*, *5*(2), 101–110.

Payette, S., Fortin, M. J., & Gamache, I. (2001). The subarctic forest-tundra: The structure of a biome in a changing climate. *Bioscience*, *51*(9), 709–718.

Payette, S., & Gagnon, R. (1985). Late Holocene deforestation and tree regeneration in the forest–tundra of Quebec. *Nature*, *313*, 570–572.

Potapov, P., Yaroshenko, A., Turubanova, S., Dubinin, M., Laestadius, L., Thies, C., et al. (2008). Mapping the world's intact forest landscapes by remote sensing. *Ecology and Society*, *13*(2), 51. URL:http://www.ecologyandsociety.org/vol13/iss2/art51/.

Ranson, K. J., Sun, G., Kharuk, V. I., & Kovacs, K. (2004). Assessing tundra–taiga boundary with multi-sensor satellite data. *Remote Sensing of Environment*, *93*, 283–295.

Rees, G., Brown, I., Mikkola, K., Virtanen, T., & Werkman, B. (2002). How can the dynamics of the tundra–taiga boundary be remotely monitored? *Ambio*, 56–62.

Serreze, M. C., Walsh, J. E., Chapin, F. S., III, Osterkamp, T., Dyurgerov, M., Romanovsky, V., et al. (2000). Observational evidence of recent change in the northern high-latitude environment. *Climate Change*, *46*, 159–207.

Skre, O., Baxter, R., Crawford, R. M. M., Callaghan, T. V., & Fedorkov, A. (2002). How will the tundra–taiga interface respond to climate change? *Ambio*, *12*, 37–46.

Swann, A. L., Fung, I. Y., Levis, S., Bonan, G. B., & Doney, S. C. (2010). Changes in Arctic vegetation amplify high-latitude warming through the greenhouse effect. *Proceedings of the National Academy of Sciences*, *107*(4), 1295–1300.

Tape, K., Sturm, M., & Racine, C. (2006). The evidence for shrub expansion in Northern Alaska and the Pan-Arctic. *Global Change Biology*, *12*, 686–702.

Timoney, K. P., La Roi, G. H., Zoltai, S. C., & Robinson, A. L. (1992). The high subarctic forest–tundra of northwestern Canada: Position, Width, and Vegetation Gradients in relation to climate. *Arctic*, *45*(1), 1–9.

Walker, D. A., Raynolds, M. K., Daniels, F. J. A., Einarsson, E., Elvebakk, A., Gould, W. A., et al. (2005). The Circumpolar Arctic vegetation map. *Journal of Vegetation Science*, *16*, 267–282.

Walker, M. D., Wahren, C. H., Hollister, R. D., et al. (2006). Plant community responses to experimental warming across the tundra biome. *Proceedings of the National Academy of Sciences*, *103*, 1342–1346.

Wulder, M. A., White, J. C., Cranny, M., Hall, R. J., Luther, J. E., Beaudoin, A., et al. (2008). Monitoring Canada's forests. Part 1: Completion of the EOSD land cover project. *Canadian Journal of Remote Sensing*, *34*(6), 549–562.

Zhou, L. M., Tucker, C. J., Kaufmann, R. K., Slayback, D., Shabanov, N. V., & Myneni, R. B. (2001). Variations in northern vegetation activity inferred from satellite data of vegetation index during 1981 to 1999. *Journal of Geophysical Research-Atmospheres*, *106* (D17), 20069–20083.